PCCP

PAPER

View Article Online
View Journal | View Issue

Cite this: *Phys. Chem. Chem. Phys.*, 2017, **19**, 7390

Spin relaxation studies of Li^+ ion dynamics in polymer gel electrolytes†

M. Brinkkötter,[a] M. Gouverneur,[a] P. J. Sebastião,[b] F. Vaca Chávez[c] and M. Schönhoff*[a]

Received 22nd December 2016,
Accepted 14th February 2017

DOI: 10.1039/c6cp08756f

rsc.li/pccp

Two ternary polymer gel electrolyte systems are compared, containing either polyethylene oxide (PEO) or the poly-ionic liquid poly(diallyldimethylammonium) bis(trifluoromethyl sulfonyl)imide (PDADMA-TFSI). Both gel types are based on the ionic liquid 1-butyl-1-methylpyrrolidinium bis(trifluoromethyl sulfonyl)imide (P_{14}TFSI) and LiTFSI. We study the influence of the polymers on the local lithium ion dynamics at different polymer concentrations using ^{7}Li spin–lattice relaxation data in dependence on frequency and temperature. In all cases the relaxation rates are well described by the Cole–Davidson motional model with Arrhenius dependence of the correlation time and a temperature dependent quadrupole coupling constant. For both polymers the correlation times are found to increase with polymer concentration. The activation energy of local motions slightly increases with increasing PEO concentration, and slightly decreases with increasing PDADMA-TFSI concentration. Thus the local Li^+ motion is reduced by the presence of either polymer; however, the reduction is less effective in the $PDADMA^+$ samples. We thus conclude that mechanical stabilization of a liquid electrolyte by a polymer can be achieved at a lower decrease of Li^+ motion when a cationic polymer is used instead of PEO.

1. Introduction

One of the key challenges of our time is the development of new energy storage systems. Problems of today's lithium-ion-batteries are the lack of stability, leakage, high vapor pressure and flammability of the organic solvent employed in the electrolyte.[1] As alternatives new electrolytes like ionic liquids are investigated.[2–4] According to the definition ionic liquids are liquid below 100 °C; thus there is still the problem of a possible leakage. The use of solid polymer electrolytes (SPE) is one possibility to overcome this issue, but the problem of these systems is often the low conductivity.[5–7] A promising strategy is thus to combine ionic liquids and polymer electrolytes to form the so-called polymer gel electrolytes in order to combine the advantages of both systems.[8,9] Ionic liquids exhibit high conductivity because of their liquid structure and polymer electrolytes are mechanically very stable systems due to their polymer network. Prototypes of polymer gel electrolyte batteries have already been developed[10] and fundamental studies of the ion transport aim at optimizing the Li^+ mobility in spite of mechanical stability of the material.[11–14]

Most commonly, polyethylene oxide (PEO) is used in polymer electrolytes, due to the favorable interaction with the lithium ion, which leads to enhancement of salt dissociation.[15] Either one or two chains of PEO may be involved in its coordination with Li^+ ions through ether oxygens.[14] The lithium is complexed by 4–5 EO-groups, if one chain is involved, and the coordination consists of 2–3 EO-groups from each chain, if the coordination is through two chains. Diddens *et al.* calculated the distance of Li^+–O_{PEO} and Li^+–O_{TFSI}^- as around 2 Å using radial distribution functions.[16] The binding of the PEO is effective, because the polymer is a polydentate ligand. Thus the chelate effect favors the binding to the ion. The coordination structure is crown-ether like and the polymer is able to build a helical structure around lithium.[17]

Instead of using a neutral polymer, which directly coordinates to the lithium ion, another possibility is the use of a cationic polymer, which may influence the lithium ion dynamics indirectly through the interaction with the anion. Pont *et al.* investigated ternary gel electrolyte systems consisting of the cationic polymer poly(diallyldimethylammonium) ($PDADMA^+$), an ionic liquid and a lithium salt.[18] The polymer $PDADMA^+$ has good thermal properties, a wide electrochemical stability window (close to 7.0 V),[18] good mechanical properties and high chemical stability.[19] Moreover, Jeremias *et al.* showed that the corresponding monomer, DADMA-TFSI, is an ionic liquid with state of the art properties.[20] From suitable ionic liquid mixtures UV-induced polymerization of $DADMA^+$ allows the *in situ* formation of polymer electrolytes of desired composition.[20]

In view of such advantageous properties the question is whether $PDADMA^+$ can compete with PEO to form an optimal compromise in polymer gel electrolytes, where mechanical

[a] *Institute of Physical Chemistry, University of Muenster, Corrensstr. 28/30, 48149 Münster, Germany. E-mail: schoenho@uni-muenster.de*
[b] *Centre of Physics and Engineering of Advanced Materials, Instituto Superior Técnico, Universidade de Lisboa, Portugal*
[c] *FAMAF – Universidad Nacional de Córdoba & IFEG-CONICET, Córdoba, Argentina*
† Electronic supplementary information (ESI) available. See DOI: 10.1039/c6cp08756f

stability is desired while enabling high Li^+ mobility. The strategy with either polymer is rather opposite: PEO enhances Li^+ salt dissociation *via* direct coordination interaction with Li^+ and can thus enhance Li^+ transport. On the other hand, a polycation can be viewed as a competitor for the interaction with the anions, which might have indirect beneficial effects. Recently Bhandary *et al.* compared gel electrolyte systems consisting of $PDADMA^+$ or PMMA and focused on the comparison of the influence of these polymers on the ion diffusivity. They observed higher D_{Li}/D_F ratios for $PDADMA^+$ in comparison to PMMA and attributed this to a partial breaking of lithium-anion clusters caused by $PDADMA^+$.[13] This enhancement of Li^+ ion motion partly compensates the decrease of lithium diffusion caused by polymer addition.[12]

In our present work we describe the local molecular motions of the lithium ion with NMR longitudinal spin relaxation rates. We perform temperature-dependent relaxation measurements to obtain activation energies. In addition, Larmor frequency-dependent relaxation measurements are carried out to analyze different time scales. Using the combination of temperature-dependent and frequency-dependent measurements, fit attempts with different motional models underlying the spin relaxation process are performed. Analysis of the resulting motional correlation times of lithium allows a detailed comparison of the two different strategies in terms of the influence of the respective polymer type on lithium ion dynamics. We finally show that the local lithium ion motional correlation time is increased in both systems by the restrictions caused by the polymer network, but this effect is partly compensated by $PDADMA^+$ due to a decrease of the coordination strength of the anion to the lithium ion.

2. Materials and methods

Materials

The polymers poly(diallyldimethylammonium)chloride (PDADMAC, aqueous solution, 20 wt%, M_w = 100.000–200.000 g mol^{-1}), polyethylene oxide (PEO, M_v = 200.000 g mol^{-1}) and lithium-bis(trifluoromethanesulfonyl)imide (LiTFSI, ≥99%) were purchased from Sigma-Aldrich. The salt was dried for 24 h at 120 °C under vacuum before use. The ionic liquid *N*-butyl-*N*-methylpyrrolidinium-bis(trifluoromethanesulfonyl)imide (P_{14}TFSI, 98.5%) was purchased from Fluka Analytical and it was dried for 24 h at 120 °C under vacuum before use.

To synthesize PDADMA-TFSI an anion exchange was performed as described by Pont *et al.*[18] PDADMAC (20 wt%, 10 mL) was mixed with an aqueous solution of LiTFSI (0.1 mol L^{-1}, 100 mL) and stirred for 4 h. The white precipitate of PDADMA-TFSI was filtered and washed with ultrapure water (Millipore). Afterwards it was freeze-dried for one week and subsequently dried in vacuum for 48 h at 100 °C. All the chemicals were stored in a glove box under an argon atmosphere.

The components of the gel electrolyte, see Scheme 1, were mixed in a glove box and dissolved in acetone. The mixtures were stirred for 24 h and dried at 60 °C for 24 h and after that dried under vacuum at 100 °C for 48 h to remove acetone.

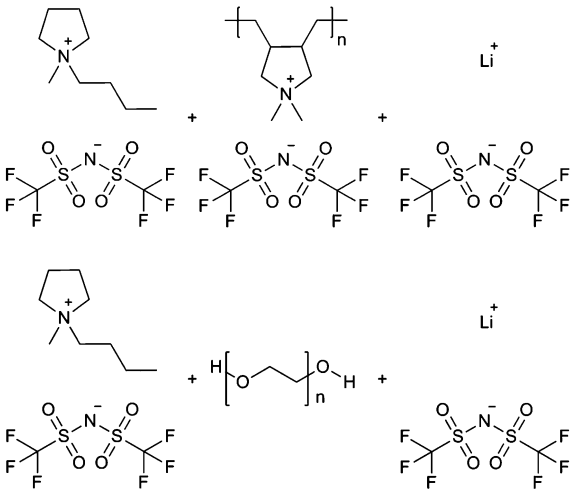

Scheme 1 Polymer gel electrolytes: top: $PDADMA^+$-based gels, bottom: PEO-based gels.

The samples were filled into the NMR-tubes in the glove box. Finally, the tubes were evacuated and then flame sealed.

The composition $x:y:z$ denotes samples with x mol P_{14}TFSI, y mol polymer (per monomer), z mol LiTFSI, and the [EO]/[Li] ratios are given in Table 1. Additionally, a reference sample without polymer was also prepared.

NMR experiments

The NMR measurements at ^{7}Li Larmor frequencies of 10.1 MHz and 26.4 MHz were performed at Instituto Superior Técnico in Lisbon on a variable field iron-core BRUKER BE-30 electromagnet operating up to 2.4 T equipped with BRUKER probe arms. The temperature was controlled using a copper/constantan thermocouple with a precision of 0.3 °C. NMR measurements at 155.5 MHz were performed at the University of Münster on a BRUKER AVANCE 400 spectrometer. The probe head "Diff30" with a variable temperature RF-coil insert for ^{7}Li (BRUKER) was used. The temperature was controlled using a GMH 3710 controller with a PT100 thermocouple (Greisinger Electronics, Germany). For all frequencies, the inversion-recovery pulse sequence was chosen for the longitudinal spin relaxation measurements. In all cases the raw data are well described by a single exponential (eqn (1)), where T_1 is the longitudinal relaxation time, t the variable delay and M_z the magnetization. The resulting T_1 values were reproducible within 5% error. The fitting of temperature- and frequency-dependent relaxation rates was done using a non-linear least squares minimization method and a web-browser interface provided by FITTEIA.[21]

$$M_z = M_z^0\left[1 - 2\exp\left(-\frac{t}{T_1}\right)\right] \quad (1)$$

Table 1 [EO]/[Li] ratio for the gel electrolyte samples containing PEO

Sample	[EO]/[Li] ratio	Sample	[EO]/[Li] ratio
PEO 20 : 02 : 4	1 : 2	PEO 04 : 20 : 4	10 : 2
PEO 20 : 10 : 4	5 : 2	PEO 20 : 15 : 2	15 : 2
PEO 20 : 20 : 4	10 : 2	PEO 20 : 20 : 2	20 : 2

Theory: BPP and CD model

To analyze the relaxation rate in more detail, the motional correlation time τ_c was calculated using the model of Bloembergen, Purcell and Pound (BPP).[22] The BPP model assumes an isotropic and random motion with one correlation time τ_c. The correlation time can describe different types of motions; for example, for ^{7}Li these may be random translational jumps. The BPP model is valid in the Redfield limit $\tau_c \ll T_{1,2}$ and is based on an exponential autocorrelation function. The Fourier transform of this correlation function gives the spectral density $J(\omega)$. The real part of the Fourier transform is a Lorentzian function of the frequency (eqn (2)).

$$J(\omega) = \int_0^\infty G(\tau)\exp(-i\omega\tau)\mathrm{d}\tau = \frac{\tau_c}{1+\omega^2\tau_c^2} \quad (2)$$

The relaxation rate R_1 can be described by eqn (3):

$$R_1 \equiv \frac{1}{T_1} = A(J(\omega_0) + 4J(2\omega_0)) \quad (3)$$

A is a prefactor containing the coupling constant of the nucleus. With the assumptions of a BPP model, eqn (2) and (3) give eqn (4):

$$R_1 = \frac{1}{T_1} = A\left(\frac{\tau_c}{1+\omega_0^2\tau_c^2} + \frac{4\tau_c}{1+4\omega_0^2\tau_c^2}\right) \quad (4)$$

If quadrupolar interaction is dominating the spin relaxation processes, the prefactor A depends on the local interaction of the ^{7}Li quadrupole moment with the electric field gradients. The prefactor can describe the symmetry of the environment of the nuclei.[23] When the electric field gradient (EFG) is axially symmetric, A can be described by eqn (5):[23]

$$A_{\mathrm{quad}} = \frac{3\pi}{100}\frac{2I+3}{I^2(2I-1)}Q^2 \quad (5)$$

In this expression Q is the quadrupole coupling constant, I the spin quantum number and η_A the asymmetry parameter of the EFG. If dipolar relaxation is relevant as a mechanism for spin relaxation, the corresponding prefactor A is

$$A_{\mathrm{dipol}} = \frac{9\mu_0^2\gamma^4\hbar^2}{128\pi^2 r^6} \quad (6)$$

Here, μ_0 is the magnetic permittivity constant, γ the gyromagnetic ratio, $\hbar$ the reduced Planck constant and r describes the distance to other nuclei. Independent of the relaxation mechanism, according to eqn (4) the maximum value of R_1 is achieved when

$$\omega_0\tau_c \approx 0.616. \quad (7)$$

With the R_1 value at the maximum the prefactor A can be calculated from eqn (4). Assuming an Arrhenius behavior of the correlation time, τ_0 and the activation energy E_A can be determined using eqn (8):

$$\tau_c = \tau_0\exp\left(\frac{E_A}{RT}\right) \quad (8)$$

In many cases, however, the BPP model does not explain the experimental results. An alternative approach, the Cole–Davidson (CD) model, assumes a distribution of correlation times.[24,25] The corresponding spectral density is given by eqn (9):

$$J_{\mathrm{CD}} = \frac{2}{\omega_0}\left[\frac{\sin\left(\varepsilon\arctan\left(\omega_0\tau_{c,\mathrm{CD}}\right)\right)}{\left(1+\omega_0^2\tau_{c,\mathrm{CD}}^2\right)^{\frac{\varepsilon}{2}}}\right] \quad (9)$$

where the exponent ε ($0 < \varepsilon < 1$) describes the width of the distribution. If the nucleus in question might exist in several sites with different mobility, superpositions of CD and/or BPP contributions may yield a suitable description of relaxation data. Alternatively, spin relaxation can even be described with further motional models, which are not used in this work (see the overview given by Beckmann[25]). The fitting of the data was done using the FITTEIA software.[21]

3. Results and discussion

To gain information about the local lithium ion dynamics and about the local activation energy, temperature and frequency dependent T_1 measurements were performed. The inversion recovery curves can be well fitted with a single exponential. As the lithium ions can be coordinated by different numbers of $TFSI^-$-anions, it can be assumed that there is not only one environment of the lithium ions. Thus it can be concluded that a fast exchange averaged environment and averaged correlation times are observed.

In Fig. 1 temperature dependent relaxation rates R_1 of ^{7}Li are shown. The results corresponding to the PEO samples at three different frequencies (10.1 MHz (a), 26.4 MHz (b), 155.5 MHz (c)) are shown at the top, and the $PDADMA^+$ measurements at the same frequencies are shown at the bottom. The maximum of R_1 is observable in the measured temperature range for all samples.

The correlation time of a Li nucleus can be quantified *via* the relaxation rate maximum $R_{1,\mathrm{max}}$.[26] Variations of the value of $R_{1,\mathrm{max}}$ indicate a change of the value of the prefactor, which can be attributed to changes of the chemical environment of the nucleus. If $R_{1,\mathrm{max}}$ is shifted to lower temperatures, the motional correlation time is decreased and if $R_{1,\mathrm{max}}$ is shifted to higher temperatures, the correlation time is increased.

PEO-based gel electrolytes

We will first turn to the results for the PEO-based gels and discuss them qualitatively. The [EO] : [Li] ratio is given in Table 1 for the different polymer concentrations.

At lower frequencies (Fig. 1a and b) $R_{1,\mathrm{max}}$ is not shifting if PEO is added, indicating that the local ion mobility is not changing. Moreover $R_{1,\mathrm{max}}$ is increasing for higher polymer contents which indicates a change of the local environment. $R_{1,\mathrm{max}}$ is hardly changing if the samples 20 : 20 : 4 PEO and 4 : 20 : 4 PEO are compared, which implies that the local environment is mainly influenced by the [EO] : [Li] ratio.

Without polymer, it can be expected that the lithium ion is coordinated by the oxygens of the anions. If PEO is added, this coordination can be partially replaced by the ethylene oxide groups and as a result the local environment is changing.

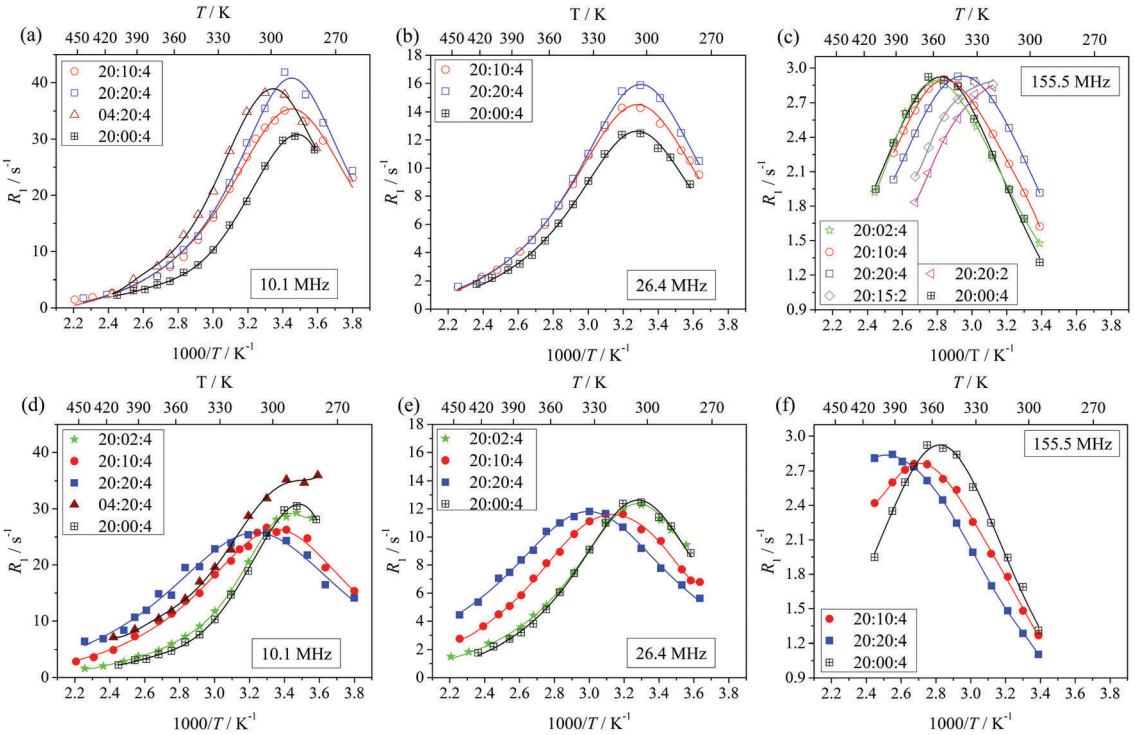

Fig. 1 Temperature dependent lithium relaxation rates R_1 at different frequencies. PEO based gels at 10.1 MHz (a), at 26.4 MHz (b) and at 155.5 MHz (c). $PDADMA^+$ based gels at 10.1 MHz (d), at 26.4 MHz (e) and at 155.5 MHz (f). The composition $x:y:z$ denotes samples with x mol $P_{14}TFSI$, y mol polymer, and z mol LiTFSI. The lines are guides to the eyes.

If quadrupolar relaxation is assumed, these changes can be attributed to variations of the EFG. Without polymer the lithium ion is probably rather symmetrically coordinated by the anions.

If PEO is added, the polymer chain is also coordinating to Li^+, which can lead to an asymmetric coordination, changing the EFG at the site of the Li ion and thus leading to an increase of $R_{1,max}$. This is in agreement with contact ion pairs coordinated to PEO, which are discussed by Kunze *et al.* in salt-in-polymer electrolyte systems.[27]

At the two low frequencies no shift and an increase of $R_{1,max}$ is observed with increasing polymer concentration. However, at 155.5 MHz (Fig. 1c), $R_{1,max}$ is not increasing with polymer concentration indicating that the local environment is not changing, whereas the position of $R_{1,max}$ is shifted to lower temperatures showing that the lithium correlation time is decreasing for increasing polymer concentrations. Such a shift of $R_{1,max}$ with increasing polymer content was also observed by Chung *et al.* at 104.6 MHz by analyzing different polymer concentrations in PEO–LiTFSI systems[28] and by Gorecki *et al.* at 95 MHz by studying a polypropylene glycol $LiCF_3SO_3$ system.[29]

The data of the sample 20 : 02 : 4 PEO at 155.5 MHz are quite similar to the data of the reference sample. This means that small amounts of polymer at an [EO] : [Li] ratio of 1 : 2 do not have a significant influence on the local environment of the lithium ion.

The effects of increasing polymer concentration at 155.5 MHz are in contrast to those at 10.1 MHz and at 26.4 MHz. At 155.5 MHz $R_{1,max}$ is shifting with an increasing polymer concentration indicating a change of the local mobility and at the lower frequencies $R_{1,max}$ is increasing without a significant shift, implying a change of the local environment. A possible explanation of this contrast is that at different frequencies different molecular motions are detected which are influenced to a different extent by the polymer.

$PDADMA^+$-based gel electrolytes

The relaxation data of the samples containing PDADMA-TFSI are shown at the bottom of Fig. 1. The samples were measured at 10.1 MHz (d), 26.4 MHz (e) and 155.5 MHz (f). At each frequency, $R_{1,max}$ is only slightly decreasing with increasing polymer content and thus the local environment of the lithium ion is only slightly changing. Furthermore, $R_{1,max}$ is shifted to higher temperatures for increasing polymer content indicating that the correlation time is increasing. At low polymer concentrations (20 : 02 : 4 PDADMA) this trend is not yet pronounced, implying a negligible influence of the polymer.

If a high amount of polymer with the composition 04 : 20 : 4 is used, $R_{1,max}$ is increased indicating that the local environment is changing. This might indicate a disturbance of the lithium $TFSI^-$ interaction by the presence of a high polymer concentration. Due to its positive charge, no direct lithium coordination is expected for $PDADMA^+$. Although the lithium ion is still coordinated by the oxygens of the $TFSI^-$ anion, an indirect influence of the cationic polymer on the lithium ion through the interaction with the anion can be expected. Therefore $PDADMA^+$ can change the structure of lithium $TFSI^-$ clusters and thus change the local mobility of the lithium ion and even slightly change the local environment.

As the polymer $PDADMA^+$ has nearly the same structure as the cation of the ionic liquid, changes of the local interactions

can be attributed to steric restrictions of the monomers caused by the polymer chain. A similar general trend of the shift of $R_{1,\max}$ in dependence of the polymer concentration was also observed by Gouverneur *et al.* at 155.5 MHz.[12]

Data analysis by the BPP or CD model

To obtain information about the activation energy and the correlation time, temperature-dependent relaxation rates were fitted using either the BPP or the CD model. To fit the ^{7}Li relaxation rates an Arrhenius behavior for the correlation time or alternatively a Vogel–Fulcher–Tammann (VTF)[30] behavior was assumed. Better results were obtained using Arrhenius behavior, and thus all following fits were performed assuming this type of temperature dependence for the correlation time.

The global fit of the ^{7}Li relaxation data of the reference sample is shown in Fig. 2. The data were fitted using the same parameters of the BPP model (A, E_A, τ_0) for the three frequencies (see eqn (4) and (8)). The agreement of the measured data and the fit is insufficient, which is mainly due to an increased or decreased maximum of the fit in comparison to the measured data. The same trend is also observed for the other samples.

Another possibility is to fit the data with the Cole–Davidson model, eqn (9). As shown in Fig. 3, the deviation of the fit and the measured data is again large. ^{7}Li has a spin quantum number of I = 3/2 and so possesses a quadrupole moment. Therefore both dipolar and quadrupolar relaxation might contribute to spin relaxation. We tried to use models including dipolar relaxation or cross relaxation to fit the data, but it was not possible to obtain reasonable results with these assumptions (see ESI,† Sections B and C). Furthermore, in the literature, in similar systems quadrupolar relaxation is known to be the dominant mechanism for ^{7}Li spin relaxation.[28,31,32]

Data analysis with temperature dependence of the chemical environment

As shown in Fig. 2 and 3 the main mismatch between the fit and the data is given by an increasing or decreasing maximum.

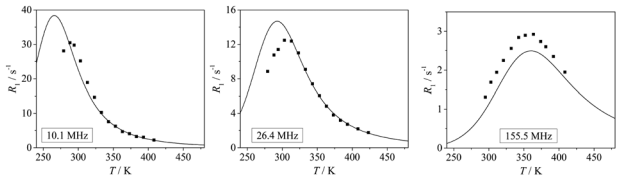

Fig. 2 R_1 data of the reference sample 20 : 00 : 4 and global fit for all frequencies with the BPP model.

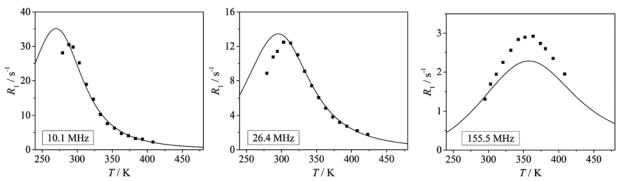

Fig. 3 R_1 data of the reference sample 20 : 00 : 4 and global fit for all frequencies with the CD model.

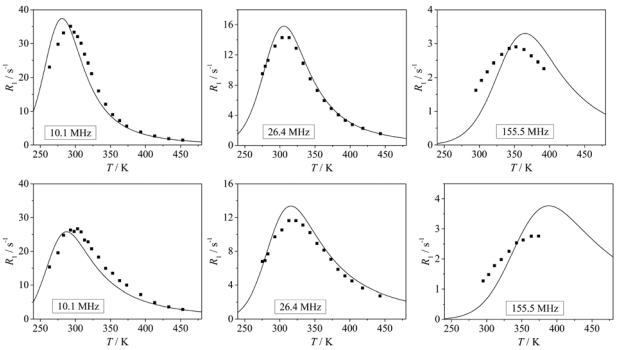

Fig. 4 R_1 data of the samples 20 : 10 : 4 PEO (top) and 20 : 10 : 4 PDADMA (bottom) and global fit for all frequencies with the BPP model of the data. The linear temperature dependence of A_{quad} is used to fit the data.

Therefore a temperature dependent prefactor A_{quad} is introduced into the model. A_{quad} is mainly influenced by the chemical environment and thus its temperature dependence implies temperature dependence of the chemical environment. As the maximum is shifted to higher temperatures, one might expect changes of the chemical environment due to breaking of clusters and changes of the intermolecular environment at higher temperatures.

In Fig. 4 the BPP fits of the data of the samples 20 : 10 : 4 PEO and 20 : 10 : 4 PDADMA are shown as an example using the linear temperature dependence of A_{quad}. Additionally, we tested exponential and also sigmoidal temperature dependence of A_{quad}, but the best results were obtained using the linear temperature dependence $A_{quad} = a \cdot T + b$, where a and b are also adjustable parameters.

CD model including a temperature dependent prefactor

The fitting can be further improved if the CD model with a temperature dependent prefactor is used. The fits for the samples 20 : 10 : 4 PEO and 20 : 10 : 4 PDADMA are shown in Fig. 5 as an example. The fits of the other samples can be found in the ESI,† Section A.

As shown, the fit of the data is further improved with this model indicating that the chemical environment of the nucleus depends on the temperature and that a distribution of environments of the nucleus is observed. The values obtained for A_{quad} and the temperature dependent quadrupolar coupling constant Q are given in Table 2.

Although in liquids one would expect a decrease of the quadrupole coupling constant with the increase of the temperature due to the averaging at higher temperatures, an increase of the coupling constant in the range of 0.01–0.08 kHz K^{-1} was observed in this work as a result of the variation of A_{quad} with temperature. Although unexpected, in the literature similar coupling constant increase effects have already been described for other systems: Ludwig *et al.* had found a linear increase of the deuteron quadrupole coupling constant of water in a water and dimethyl sulfoxide mixture of 0.08 kHz K^{-1} in the temperature range from 188 K to 308 K.[33] In liquid ammonia a linear temperature dependence of 0.1 kHz K^{-1} was determined by Hardy *et al.* for the deuteron quadrupole coupling constant in the temperature

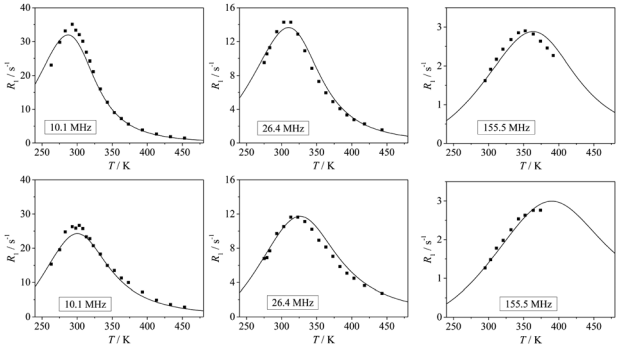

Fig. 5 R_1 data of the samples 20 : 10 : 4 PEO (top) and 20 : 10 : 4 PDADMA (bottom) and global fit for all frequencies with the CD model of the data. The linear temperature dependence of A_{quad} is used to fit the data.

range from 237 K up to 293 K.[34] A linear temperature dependence of the ^{7}Li quadrupolar coupling constant of 0.05 kHz K^{-1} above 330 K was found by Arun *et al.* in an intercalated polymer electrolyte (IPE), $Cd_{0.75}PS_3Li_{0.5}$(PEO).[35]

Further examples of the increase of the quadrupole coupling constant in liquids can be found elsewhere.[36,37]

The increase of the quadrupole coupling constant with temperature can be explained by different mechanisms. Halstead proposed that an increase of the quadrupole coupling constant may occur for light atoms, since temperature determines the range of different coordination environments that are thermally sampled.[38] The EFG might vary in the region around the nucleus and therefore the time average might depend on the region in which the nucleus moves. As the Brownian motion of the nucleus is temperature dependent the time average of the electric field gradient might be temperature dependent and as a result also the quadrupole coupling constant.

On the other hand, Arun *et al.* explained the temperature-dependence of A by changes in the time average of the EFG using an anisotropic quantum oscillator model.[35] Other possible explanations are a change of the EFG induced by a change of the atomic coordinates or induced by a change of the electron density distribution.[39]

In our system, a change of the electron density distribution might occur, induced by a change of the coordination structure of the lithium ion. If at higher temperatures the distance of certain nearest neighbors to the lithium ion is reduced, steric hindrance might increase the distance of other nearest neighbors to the lithium ion, which would increase the asymmetry of the coordination. Therefore the temperature dependence of A_{quad} might be induced not only by the temperature dependence of the quadrupolar coupling constant, but also by the slight temperature dependence of the asymmetry parameter.

The lowest prefactor was found in the reference sample (see Table 2) indicating a more isotropic coordination of the lithium ion in comparison to the samples with polymer. A_{quad} was found to increase with increasing polymer concentrations, which implies that the symmetry of the lithium coordination decreases when polymer is added. Chung *et al.* measured a polypropylene oxide sample with different amounts of $LiCF_3SO_3$ and calculated the values of A_{quad} from 2.6 × 10^9 s^{-2} up to 3.4 × 10^9 s^{-2} assuming BPP behavior of ^{7}Li spin relaxation.[28] The order of magnitude and the trend with increasing polymer content are very similar to our system (see Table 2).

CD and BPP contribution with a temperature dependent prefactor

The quality of the fit can be further improved by a model involving superposition of the CD and BPP contribution, each including a temperature dependent prefactor A_{quad} (see ESI,† Section D). The resulting parameters are given in Tables S2–S5 (ESI†). For all polymer samples, the CD contribution is the dominant one (compare the respective values of A_{quad} in Table S2 (ESI†) to those of the BPP contribution in Table S4 (ESI†)). The trend of the parameters describing this dominant CD contribution (see Table S3, ESI†) is in agreement with that of the model employing only the CD contribution (see Table 3). For the BPP part of the fit the contribution to the relaxation rate is low and therefore the quality of these fitting results might be insufficient.

As for the reference sample, a very good fit can already be obtained with one CD contribution including a temperature dependent prefactor, see Fig. S1 (ESI†), or with two BPP contributions, see data in Table S3 (ESI†) with $\varepsilon = 1$; thus using CD and BPP contribution will overparametrize the relaxation data.

We conclude that in the polymer samples there might be a minor contribution of Li in a site with different correlation times, leading to a slight deviation of the CD fit from the data in Fig. 5 and Fig. S1 (ESI†), but its contribution to the relaxation rate is too small to allow for a detailed analysis. Thus, we restrict the discussion to the fit parameters of the CD model given in Table 3.

Interpretation of the ^{7}Li dynamics

The values of the activation energy E_A, the correlation time τ_0 and the factor ε obtained from the CD model with a temperature-dependent prefactor are presented in Table 3. The width parameter

Table 2 Fit parameters a, b and the temperature-dependent prefactor $A_{quad} = a \cdot T + b$ for the CD model. As examples, values of A_{quad} at 298 K (A_{298}) and at 373 K (A_{373}) are shown. The quadrupolar coupling constant Q is calculated at 298 K and 373 K

Sample	a/s^{-2} K^{-1}	b/s^{-2}	A_{298}/s^{-2}	Q_{298}/kHz	A_{373}/s^{-2}	Q_{373}/kHz
20 : 00 : 4 reference	4.9 × 10^6	−8.1 × 10^8	6.5 × 10^8	11	1.0 × 10^9	14
20 : 10 : 4 PEO	4.8 × 10^6	−4.6 × 10^8	9.7 × 10^8	14	1.6 × 10^9	18
20 : 20 : 4 PEO	4.8 × 10^6	−2.9 × 10^7	1.4 × 10^9	17	1.6 × 10^9	18
20 : 10 : 4 PDADMA	8.8 × 10^6	−1.7 × 10^9	8.9 × 10^8	13	1.3 × 10^9	16
20 : 20 : 4 PDADMA	9.4 × 10^6	−1.9 × 10^9	9 × 10^8	13	1.8 × 10^9	19

Table 3 Values of the width parameter ε, the activation energy E_A and correlation time t using the CD model with a temperature dependent prefactor. As examples, values of the correlation time τ_0 at 298 K (τ_{298}) and at 373 K (τ_{373}) are given

Sample	ε	τ_0/s	E_A/kJ mol^{-1}	τ_{298}/s	τ_{373}/s
20 : 00 : 4 reference	0.43	2.6×10^{-14}	31	6.4×10^{-9}	5.3×10^{-10}
20 : 10 : 4 PEO	0.25	3.6×10^{-14}	32	1.3×10^{-8}	1.7×10^{-9}
20 : 20 : 4 PEO	0.16	4.2×10^{-14}	32	1.6×10^{-8}	3.0×10^{-9}
20 : 10 : 4 PDADMA	0.19	1.5×10^{-13}	29	1.8×10^{-8}	9.7×10^{-10}
20 : 20 : 4 PDADMA	0.16	4.1×10^{-13}	28	2.9×10^{-8}	1.2×10^{-9}

ε describes the distribution of the correlation time. If ε is lower, the distribution of the correlation time is broader.

The value of ε is decreasing for increasing polymer concentration, which can be attributed to an increasing heterogeneity of cluster structures with increasing polymer content. Since for the PDADMA$^+$ samples it is expected that the lithium ions remain coordinated by the oxygens of the anions independent of the polymer concentration, the heterogeneity might be caused by polymer induced steric constraints on the local ionic arrangement, modifying for example neighbor distances. As a result these constraints increase the distribution width of lithium ion correlation times.

For the PEO samples the increasing heterogeneity might be induced more directly by the polymer, since lithium ions are coordinated probably by varying numbers of ethylene oxide groups and anions, respectively. Thus PEO not only changes the EFG of the lithium environment, due to the replacement of the anions by the ethylene oxide groups, but also increases the heterogeneity of the local lithium ion mobility. The activation energy of the lithium is only slightly increasing if PEO is added, indicating that the addition of PEO is not strongly influencing the local characteristics. The correlation time is increasing if PEO is added which might be attributed to the restriction of the movement caused by the polymer network. Similarly, an increase of the correlation time was also observed for the PDADMA$^+$ system. There, the increase of the correlation time was already indicated by the shift of $R_{1,\max}$ in dependence of the polymer concentration. The increase of τ_0 for higher amount of polymer can be attributed to the restriction of the movement caused by the chains.

In spite of the increase of the correlation time, the activation energy is decreasing with increasing PDADMA$^+$ concentrations. This might be caused by the ability of PDADMA$^+$ to interact with the anion and thereby locally change the lithium anion cluster structure, which might decrease the activation energy. This seemingly ambiguous result of a decrease of the activation energy and a simultaneous increase of the correlation time might be attributed to the restrictions caused by the polymer. The correlation time τ_c is increasing as the decrease of the activation energy only partly compensates the increase of the correlation time caused by the restriction by the polymer. The increase of τ_c indicates that in addition to the long range dynamics the local ion dynamics is also affected by the polymer chains.

Previously, by assuming a BPP behavior for the temperature dependent spin lattice relaxation rate, Gouverneur *et al.* had obtained for ^{7}Li an increase of the correlation time and a decrease of the activation energy for increasing PDADMA$^+$ concentrations at 155.5 MHz which is consistent with our findings.[12]

Bhandary *et al.* compared the polymer effect of two types of polymers, a cationic and an acrylate polymer, on the lithium ion transport in liquid electrolytes by diffusion measurements.[13] The data implied a breaking of lithium TFSI$^-$ clusters upon PDADMA$^+$ addition and therefore PDADMA$^+$ was found to partly compensate the reduction of the lithium ion diffusivity induced by viscosity enhancement following polymer addition. In conclusion, PDADMA$^+$ was considered a more suitable polymer than PMMA for combining high Li$^+$ mobility (*i.e.* short τ_c) with mechanical stability in gel electrolyte systems.

In this work a similar comparison between a neutral, coordinating polymer (PEO) and the cationic polymer PDADMA$^+$ based on spin relaxation is presented. Our results show that the correlation time of the lithium ion is increased if either PEO or PDADMA$^+$ is added to a liquid electrolyte, due to the chain rigidity. However, the local activation energy decreases if PDADMA$^+$ is added and increases if PEO is added. This demonstrates that PDADMA$^+$ is partly compensating and PEO is not compensating the decrease of the lithium ion mobility caused by polymer addition. Our results demonstrate that PDADMA$^+$ is not only more suitable than an acrylate polymer for gel electrolyte systems, but also better suited than PEO in terms of rendering Li ions mobile in a gel system.

The activation energies shown in Table 3, obtained by ^{7}Li spin relaxation, can be compared to those reported for similar polymer gel electrolytes. Gouverneur *et al.* obtained local lithium activation energies from 15 to 20 kJ mol^{-1} in ternary PDADMATFSI systems.[12] Similar activation energies were also obtained for salt-in-polymer electrolytes. Kunze *et al.* found local lithium activation energies from 13 kJ mol^{-1} up to 18 kJ mol^{-1} in polysiloxane-based salt-in-polymer electrolytes measuring at two frequencies and using a CD model.[40] Moreover, Hayamizu *et al.* analyzed a cross-linked poly(ethylene oxide–propylene oxide) random copolymer doped with LiTFSI and found local lithium activation energies of 22.3 kJ mol^{-1} and 24.3 kJ mol^{-1}.[41] The activation energies in these systems are different from the activation energies in our gels. The differences can mainly be attributed to the choice of the frequencies and the used relaxation model. Gouverneur *et al.* and Hayamizu *et al.* used the BPP model for measurements at 155.5 MHz and 77.63 MHz, respectively. Furthermore Kunze *et al.* used the CD model for measurements at 77.7 MHz and 155.5 MHz, while in our present work the CD model with a temperature dependent prefactor is used. However, if the BPP model is applied to our experimental data obtained at 155.5 MHz, activation energies of 18 kJ mol^{-1} and 20 kJ mol^{-1} for the samples 20 : 10 : 4 PDADMA and 20 : 10 : 4 PEO are obtained, respectively. These activation energies are in agreement with data available in the literature. This shows that the local activation energy is frequency and model dependent; however, within one system, small but distinct differences between various investigated samples can be identified.

4. Conclusion

In this work we studied the influence of polymers on the local dynamics and the local environment of the lithium ion in polymer gel electrolytes using frequency and temperature dependent T_1 relaxation measurements. We compared two different types of polymers, the cationic polymer PDADMA$^+$ and the neutral polymer PEO; the latter is known to interact with Li ions in crown ether type of structures.

We were able to fit the lithium relaxation data assuming the CD model with Arrhenius behavior of the correlation times and a temperature dependent quadrupole coupling constant. The latter is modeled and is found to increase linearly with temperature. Since the correlation time of the lithium ions increased with addition of polymer, the polymer was shown to restrict the local motion of the lithium. Thus, the local Li ion dynamics is not completely decoupled from the viscosity of the samples. Local lithium activation energies between 28 kJ mol^{-1} and 32 kJ mol^{-1} were calculated for the different samples using the CD model with a temperature dependent prefactor. The local activation energy was slightly increased when PEO was added and slightly decreased in the case of addition of PDADMA$^+$. Thus, at a local scale it is more efficient to use a cationic polymer to achieve a short lithium ion correlation time, because it induces fragmentation of lithium-anion clusters, than to use a neutral polymer which can directly interact *via* coordination interaction with the lithium ion. In summary, the addition of any of these polymers leads to an increase of the local lithium ion correlation time. However, this effect is more compensated by favourable interactions in the case of PDADMA$^+$ in comparison to PEO.

Interesting further aspects concern the local environment of the lithium ion as interpreted from temperature-dependent values of A_{quad}. With polymer addition, the local lithium ion coordination equilibrium becomes more heterogeneous and the anisotropy of the lithium environment is further enhanced by temperature.

Acknowledgements

We acknowledge the financial support of the DAAD in the international exchange program "Projektbezogener Personenaustausch mit Portugal – Acções Integradas Luso-Alemãs". Marc Brinkkötter is supported by a stipend of the "Fonds der Chemischen Industrie" (FCI, Germany).

References

1 B. Scrosati and J. Garche, *J. Power Sources*, 2010, **195**, 2419–2430.
2 A. Balducci, S. S. Jeong, G. T. Kim, S. Passerini, M. Winter, M. Schmuck, G. B. Appetecchi, R. Marcilla, D. Mecerreyes, V. Barsukov, V. Khomenko, I. Cantero, I. De Meatza, M. Holzapfel and N. Tran, *J. Power Sources*, 2011, **196**, 9719–9730.
3 A. Lewandowski and A. Świderska-Mocek, *J. Power Sources*, 2009, **194**, 601–609.
4 H. Kim, Y. Ding and P. A. Kohl, *J. Power Sources*, 2012, **198**, 281–286.
5 M. B. Armand, *Annu. Rev. Mater. Sci.*, 1986, **16**, 245–261.
6 W. H. Meyer, *Adv. Mater.*, 1998, **10**, 439–448.
7 M. Armand, *Solid State Ionics*, 1994, **69**, 309–319.
8 A. Manuel Stephan, *Eur. Polym. J.*, 2006, **42**, 21–42.
9 J. Y. Song, Y. Y. Wang and C. C. Wan, *J. Power Sources*, 1999, **77**, 183–197.
10 G. T. Kim, S. S. Jeong, M. Z. Xue, A. Balducci, M. Winter, S. Passerini, F. Alessandrini and G. B. Appetecchi, *J. Power Sources*, 2012, **199**, 239–246.
11 J. Chattoraj, D. Diddens and A. Heuer, *J. Chem. Phys.*, 2014, **140**, 024906.
12 M. Gouverneur, S. Jeremias and M. Schönhoff, *Electrochim. Acta*, 2015, **175**, 35–41.
13 R. Bhandary and M. Schönhoff, *Electrochim. Acta*, 2015, **174**, 753–761.
14 D. Diddens and A. Heuer, *ACS Macro Lett.*, 2013, **2**, 322–326.
15 Z. Xue, D. He and X. Xie, *J. Mater. Chem. A*, 2015, **3**, 19218–19253.
16 D. Diddens and A. Heuer, *J. Phys. Chem. B*, 2014, **118**, 1113–1125.
17 F. Müller-Plathe and W. F. van Gunsteren, *J. Chem. Phys.*, 1995, **103**, 4745–4756.
18 A.-L. Pont, R. Marcilla, I. De Meatza, H. Grande and D. Mecerreyes, *J. Power Sources*, 2009, **188**, 558–563.
19 G. B. Appetecchi, G. T. Kim, M. Montanino, M. Carewska, R. Marcilla, D. Mecerreyes and I. De Meatza, *J. Power Sources*, 2010, **195**, 3668–3675.
20 S. Jeremias, M. Kunze, S. Passerini and M. Schönhoff, *J. Phys. Chem. B*, 2013, **117**, 10596–10602.
21 P. J. Sebastião, *Eur. J. Phys.*, 2014, **35**, 015017.
22 N. Bloembergen, E. M. Purcell and R. V. Pound, *Phys. Rev.*, 1948, **73**, 679–712.
23 J. Kowalewski and L. Mäler, *Nuclear Spin Relaxation in Liquids: Theory, Experiments, and Applications*, Taylor & Francis Group, LLC, 2006.
24 D. W. Davidson and R. H. Cole, *J. Chem. Phys.*, 1951, **19**, 1484–1490.
25 P. A. Beckmann, *Phys. Rep.*, 1988, **171**, 85–128.
26 L. V. S. Lopes, D. C. Dragunski, A. Pawlicka and J. P. Donoso, *Electrochim. Acta*, 2003, **48**, 2021–2027.
27 M. Kunze, Y. Karatas, H. D. Wiemhöfer and M. Schönhoff, *Macromolecules*, 2012, **45**, 8328–8335.
28 S. H. Chung, K. R. Jeffrey and J. R. Stevens, *J. Chem. Phys.*, 1991, **94**, 1803–1811.
29 W. Gorecki, M. Jeannin, E. Belorizky, C. Roux and M. Armand, *J. Phys.: Condens. Matter*, 1995, **7**, 6823.
30 G. S. Fulcher, *J. Am. Ceram. Soc.*, 1925, **8**, 339–355.
31 W. R. Carper, *Concepts Magn. Reson.*, 1999, **11**, 51–60.
32 J. P. Donoso, T. J. Bonagamba, H. C. Panepucci, L. N. Oliveira, W. Gorecki, C. Berthier and M. Armand, *J. Chem. Phys.*, 1993, **98**, 10026–10036.
33 R. Ludwig, T. C. Farrar and M. D. Zeidler, *J. Phys. Chem.*, 1994, **98**, 6684–6687.
34 E. H. Hardy and M. D. Zeidler, *Phys. Chem. Chem. Phys.*, 2000, **2**, 1645–1648.

35 N. Arun, S. Vasudevan and K. V. Ramanathan, *J. Chem. Phys.*, 2003, **119**, 2849–2853.
36 M. A. Wendt, M. D. Zeidler and T. C. Farrar, *Mol. Phys.*, 1999, **97**, 753–756.
37 R. Ludwig, F. Weinhold and T. C. Farrar, *J. Phys. Chem. A*, 1997, **101**, 8861–8870.
38 T. K. Halstead, *J. Chem. Phys.*, 1970, **53**, 3427–3435.
39 T. Pietrass and P. K. Burkert, *Magn. Reson. Chem.*, 1993, **31**, 709–713.
40 M. Kunze, Y. Karatas, H. D. Wiemhöfer, H. Eckert and M. Schönhoff, *Phys. Chem. Chem. Phys.*, 2010, **12**, 6844–6851.
41 K. Hayamizu, Y. Aihara and W. S. Price, *J. Chem. Phys.*, 2000, **113**, 4785–4793.

